Liquid Crystals
Publication details, including instructions for authors and subscription information:
http://www.informaworld.com/smpp/title~content=t713926090

Analysis of cell gap-dependent driving voltage in a fringe field-driven homogeneously aligned nematic liquid crystal display

Hyang Yul Kim[ab]; Seung Ho Hong[a]; John Moon Rhee[b]; Seung Hee Lee Corresponding author[b]
[a] Development Division, BOE-HYDIS Technology Co. Ltd., Kyungki-do 467-701, Korea [b] School of Advanced Materials Engineering, Chonbuk National University, Chonbuk 561-756, Korea

Online publication date: 19 May 2010

To cite this Article Kim, Hyang Yul , Hong, Seung Ho , Rhee, John Moon and Lee Corresponding author, Seung Hee(2003) 'Analysis of cell gap-dependent driving voltage in a fringe field-driven homogeneously aligned nematic liquid crystal display', Liquid Crystals, 30: 11, 1285 — 1292
To link to this Article: DOI: 10.1080/02678290310001605893
URL: http://dx.doi.org/10.1080/02678290310001605893

LIQUID CRYSTALS, VOL. 30, NO. 11, NOVEMBER, 2003, 1285–1292

Taylor & Francis
Taylor & Francis Group

Analysis of cell gap-dependent driving voltage in a fringe field-driven homogeneously aligned nematic liquid crystal display

HYANG YUL KIM†‡, SEUNG HO HONG†, JOHN MOON RHEE‡ and SEUNG HEE LEE‡*

†Development Division, BOE-HYDIS Technology Co. Ltd., Ichon-si, Kyungki-do 467-701, Korea

‡School of Advanced Materials Engineering, Chonbuk National University, Chonju-si, Chonbuk 561-756, Korea

(*Received 27 January 2003; in final form 2 June 2003; accepted 14 June 2003*)

We have studied cell gap-dependent driving voltage characteristics in a homogeneously aligned nematic liquid crystal (LC) cell driven by a fringe electric field, termed the fringe field switching (FFS) mode. The results show that for the FFS mode using a LC with positive dielectric anisotropy, the operating voltage decreases as the cell gap decreases, whereas it increases with a decreasing cell gap when using a LC with negative dielectric anisotropy. The difference between LCs is explained by simulation and experiment.

1. Introduction

The image quality of liquid crystal displays (LCDs) has been improved greatly using several wide viewing angle technologies. Among them are in-plane switching (IPS) [1–5] and fringe field switching (FFS) [6–12] modes utilizing the concept of an in-plane rotation of the LC director. In both devices, the electrodes are on only one substrate such that, in the IPS device, the distance l between pixel and counter electrodes is always larger than that of the cell gap d and the width w of the electrodes. In contrast, in the FFS device, l is smaller than d and w, or there is no horizontal distance between them. Therefore, in the IPS device when a voltage is applied, a horizontal electric field is generated between the electrodes and the field drives the homogeneously aligned LC molecules to rotate almost in-plane. However, in the FFS mode, instead of a horizontal field, a fringe electric field that has both horizontal and vertical components controls the deformation of the LCs, and this difference causes the electro-optic characteristics of the two devices to be different from each other. For example, the light efficiency of the FFS mode depends on the dielectric anisotropy of the LCs and the rubbing angle [11], unlike in the IPS mode.

In the IPS mode, the threshold voltage V_{th} at which transmittance starts to occur is inversely proportional to d and proportional to l, and described by [4]

$$V_{th} = \pi l/d \times (K_{22}/\varepsilon_0 \Delta\varepsilon)^{1/2} \quad (1)$$

where K_{22} is the twist elastic constant and $\Delta\varepsilon$ the dielectric anisotropy of the LC. This suggests that when the cell gap decreases, the surface effect that holds LCs increases, such that a the higher driving voltage (V_{op}) is required to rotate the LCs.

In the FFS mode, we have studied voltage-dependent transmittance (V–T) characteristics depending on the cell gap. Interestingly, when a LC with negative dielectric anisotropy ($-$LC) is used, V_{op} increases with decreasing d, which is similar to that seen for the IPS mode. However, when a LC with positive dielectric anisotropy ($+$LC) is used, V_{op} decreases with decreasing d. In this paper, the field distribution and the LC director profile that account for such different electro-optic behaviour have been studied by simulation and experiment.

2. Cell structure and switching principle of the FFS mode

Figure 1 shows the electrode structure of the FFS mode on the bottom substrate. As indicated, the pixel and counter electrode with a thickness of 400 Å exist only on the bottom substrate with a passivation layer of 3000 Å thickness between them. The width of each pixel electrode is 3 μm and the distance between them is 4.5 μm, such that the distance L from the centre of a pixel to a common electrode is 3.75 μm. With this electrode structure, when a voltage is applied a fringe

*Author for correspondence;
e-mail: lsh1@moak.chonbuk.ac.kr

Liquid Crystals ISSN 0267-8292 print/ISSN 1366-5855 online © 2003 Taylor & Francis Ltd
http://www.tandf.co.uk/journals
DOI: 10.1080/0267829031000160589 3

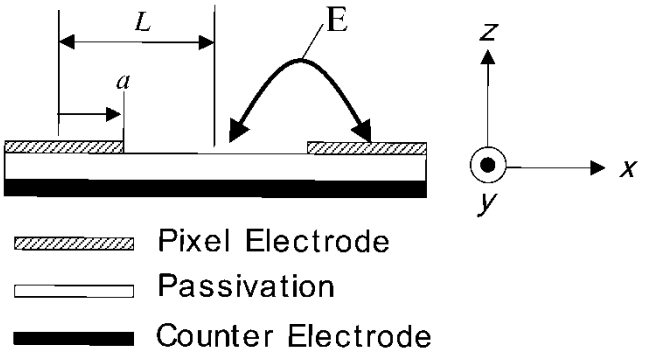

Figure 1. Cross-section view of the electrode structure on bottom substrate in the FFS mode.

electric field that has both horizontal (E_x) and vertical (E_z) components is generated.

Figure 2 shows the fringe electric field distribution of the vertical and horizontal components in the FFS device along the x-axis for a distance L and the z-axis with $d=4\,\mu m$, when the applied voltage is 5 V. Here a position of $x=0$ indicates the centre of the pixel electrode, as indicated in figure 1. As clearly shown, a strong horizontal field intensity E_x exists at the edges of the pixel electrodes (position a) near the bottom surface, whereas it weakens rapidly as it moves away from the bottom surface. Both E_x and E_z occur between the edge and the centre of the electrodes, while E_x is zero above the electrodes centre. In contrast to E_x, E_z is at a maximum between the centre and the edge of an electrode, and zero at the edge of an electrode. This field distribution in the FFS device causes the LC molecules to respond differently to an electric field depending on the dielectric anisotropy of the LCs.

Now, considering the switching behaviour of the FFS mode, the light transmittance can be described as,

$$T = T_0 \sin^2[2\alpha(V)] \sin^2(\pi d\Delta n/\lambda) \qquad (2)$$

which is similar to the IPS mode, and where α is a voltage-dependent angle between the transmission axis of the crossed polarizer and the optic axis of the LC, Δn is the phase retardation value and λ is the wavelength of the incident light. The homogenously aligned LCs with $\alpha=0^\circ$ in the initial state rotate due to a fringe electric field, giving rise to transmittance at a given phase retardation value. Figure 3 shows the LC director distribution in the white state and normalized light transmittance (T') as a function of relaxation time for the $-$LC and $+$LC. For the simulations, the commercially available software 'LCD Master' from Shintech, Japan was used, and the simulation conditions are summarized in the table. As is clearly seen in both cases, after 5 ms the LCs near the edge of the electrode (position A) respond to the field at first due to a strong E_x, giving rise to a high transmittance compared with other areas and, as time elapses further, a high transmittance occurs even at the centre of the electrode (position B). This suggests that the LCs near both edges of the electrode rotate first due to a strong E_x and then, on further increasing the time, the LCs at the centre of the electrode also rotate via a twisting elastic force between neighbouring molecules. In this way, transmittance occurs throughout the entire area of the $-$LC. However for the $+$LC, the LCs between the edge and the centre of the electrodes tilt up due to the existence of a strong E_z so that the twisting elastic force causing the rotation of the LCs at the centre of the electrode becomes weaker than that for the $-$LC, resulting in a lower transmittance than for the $-$LC. The higher upward tilt of the $+$LC than of the $-$LC at that position can be seen in the LC director distribution of figure 3 (*b*).

3. Results and discussion

Figure 4 shows calculated V–T curves for the $-$LC and the $+$LC, where the cell gap was varied from 3 to 5 μm with Δn fixed. For the $-$LC, V_{th} and the operating voltage V_{op} at which the maximum transmittance occurs are increased from 4.8 to 5.5 V on decreasing

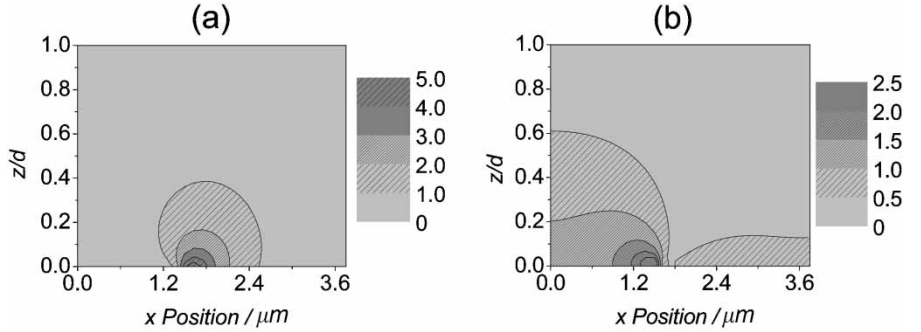

Figure 2. Distribution of (*a*) horizontal and (*b*) vertical electric fields along horizontal and vertical axes in the FFS mode. The numbers indicating the range have a unit of field intensity.

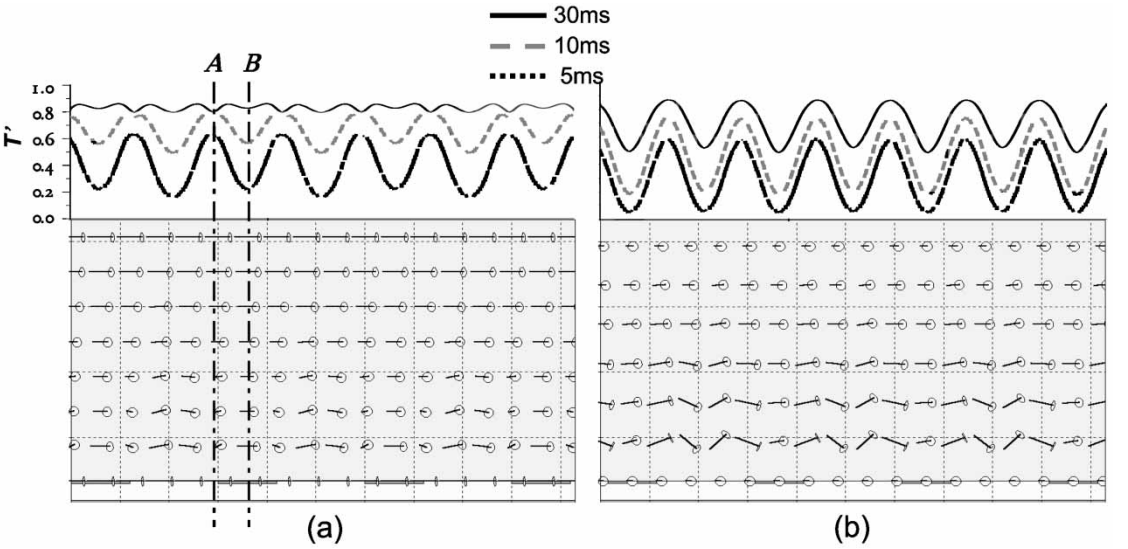

Figure 3. Transmittance profile as a function of relaxation time along the *y*-axis with the LC director profile at an operating voltage for (*a*) −LC and (*b*) +LC.

Table 1. Cell and LC parameters used for the simulations.

Parameter	Value	
Pretilt angle/°	2	
d/μm	4	
	−LC	+LC
Rubbing angle w.r.t. E_x/°	12	78
K_1/pN	13.5	9.7
K_2/pN	6.5	5.2
K_3/pN	15.1	13.3
Δn at 550 nm	0.077	0.1
$\Delta\varepsilon$	−4	8

the cell gap. This is similar to that found for the IPS mode, in which the surface anchoring effect strengthens as the cell gap becomes smaller; as a result, higher electrical energy is necessary to deform the LC. However, when the +LC is used, this trend is reversed, as revealed in figure 4 (*b*). Interestingly, V_{op} decreases on decreasing the cell gap, while V_{th} increases with a smaller cell gap as expected. Specifically, when the cell gap is 5 μm, the transmittance saturates at about 6.5 V, whereas V_{op} is only 3.7 V for the cell with $d=3$ μm. Experiments were performed to confirm these calculated results; in these experiments, −LC ($\Delta n=0.077$, $\Delta\varepsilon=-4$) and +LC ($\Delta n=0.116$, $\Delta\varepsilon=7.9$) were used and the electrode structure was the same as that in the simulation. Figure 5 shows experimental *V*–*T* curves, which show similar trends to the calculated data. For the −LC, V_{op} increased from 6.5 to 7 V and, V_{th} also increased when the cell gap was decreased from 4 to 3 μm. However, for the +LC, when the cell gap was decreased from 4 to 3 μm, V_{op} decreased from 4.3 to 4.1 V, while the V_{th} increased.

As mentioned already, the electro-optic behaviour of

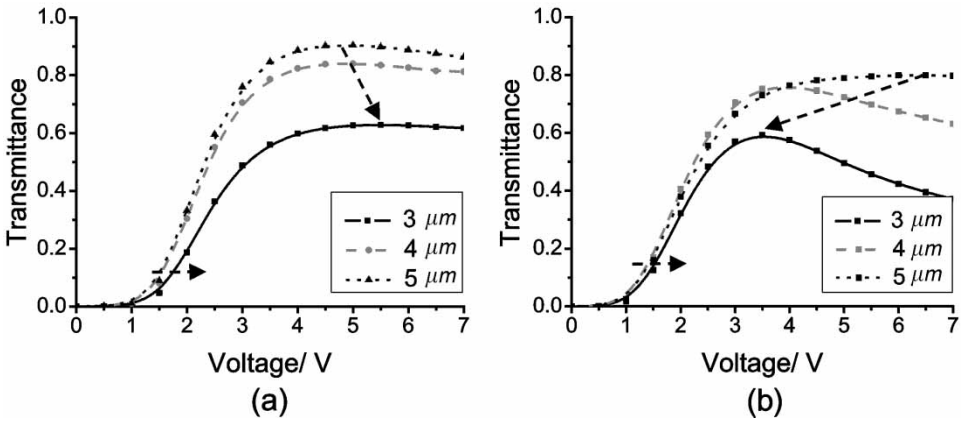

Figure 4. Calculated *V*–*T* curves for (*a*) +LC and (*b*) −LC. The arrows indicate traces of the operating and the threshold voltages.

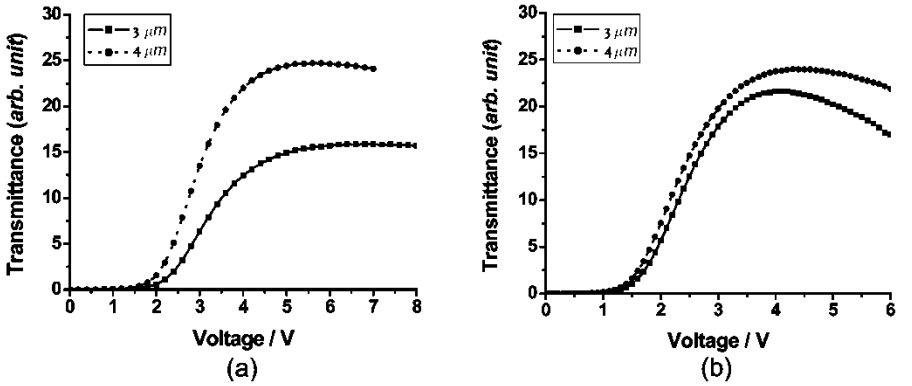

Figure 5. Experimental V–T curves for (a) +LC and (b) −LC.

the FFS mode might differ depending on the type of LCs used because the LCs are effected by a fringe electric field unlike the IPS mode with uses only an in-plane field, such that the transmittance is dependent on the electrode position. In order to understand this difference between the −LC and +LC, we have investigated the transmittance distribution and the LC director profile at different cell gaps and voltages. Figure 6 shows an iso-transmittance contour along the x-axis for distance L as a function of voltage for two different cell gaps with a −LC, where the thick dotted lines indicate the voltage that shows maximum transmittance at each position, and the scale in the inset indicates the normalized transmittance. As shown in figure 6 (a), for the smaller cell gap 3 μm, V_{op} is strongly dependent on the electrode position, and is low at the edge of the electrode and high at the centre. This results in a high V_{op} of over 5 V. However, for the larger cell gap of 5.6 μm, the positional dependency of V_{op} is not so strong; it is slightly higher at the centre of the electrode than at the edge, resulting in a V_{op} of below 5 V, as shown in figure 6 (b). In addition, and as expected from figure 3 (a), high transmittance occurs in all positions for both cases and only V_{op} is positionally dependent.

Figure 7 shows the iso-transmittance contour along the x-axis for a distance L as a function of voltage for two different cell gaps with the +LC. When the cell

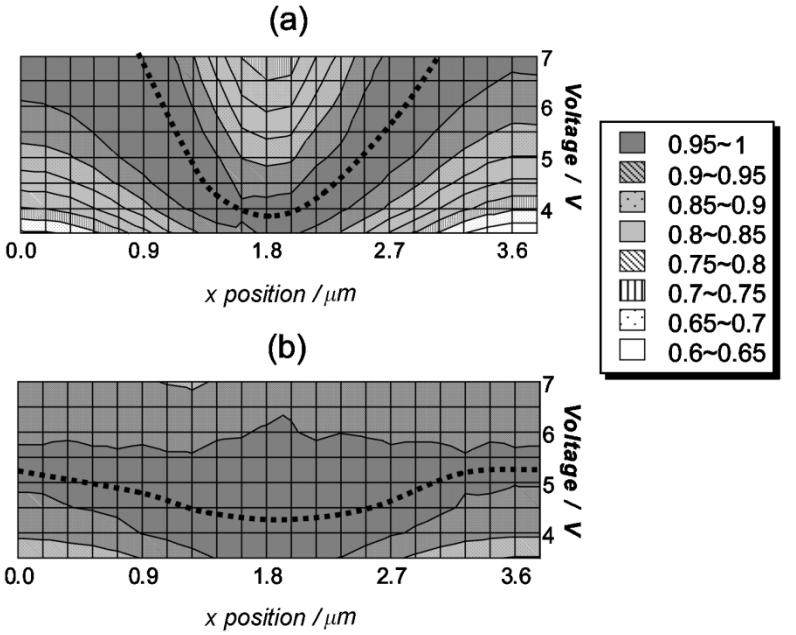

Figure 6. Transmittance distribution along the x-axis for two different cell gaps, (a) 3 μm and (b) 5.6 μm, as a function of an applied voltage when using the −LC; the thick-dotted lines indicate the voltage at which maximum transmittance occurs at each position.

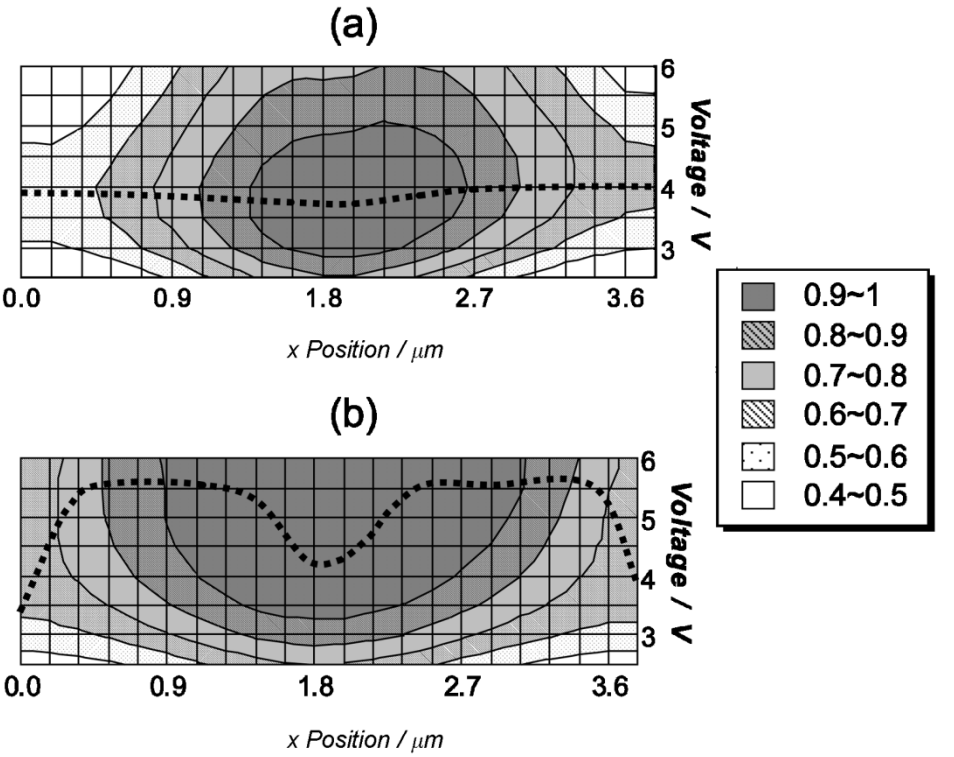

Figure 7. Transmittance distribution along the x-axis for two different cell gaps, (a) 3 μm and (b) 4.6 μm, as a function of an applied voltage when using the +LC; the thick-dotted lines indicate the voltage at which maximum transmittance occurs at each position.

gap is 3 μm, V_{op} is almost independent of position, whereas for the cell with $d=4.6$ μm, it is higher between the edge and the centre of the electrodes than when calculated. It should be noted that V_{op} is about the same at the centre of the electrodes, irrespective of the cell gap, and the transmittance is high at the edge of the electrodes compared with other positions, in both cases. From the results, we see that in the FFS mode, both V_{op} and the light transmittance are dependent on the electrode position and their behaviour depends on the dielectric anisotropy of the LC. This results in different behaviour in the cell gap-dependent V–T curve, i.e. for −LC, V_{op} is inversely proportional to the cell gap, whereas it is proportional to the cell gap for the +LC.

Next, the director profile was investigated in horizontal and vertical positions, while changing the cell gap and the applied voltage, in order to understand in detail how the LC molecules respond to a fringe electric field. Figure 8 shows the distribution of the LC director at two different voltages, 4.5 and 5.5 V, for a cell gap of 3 μm with the −LC, and the scale indicates the degree of the twist and tilt angle. Figures 8 (a) and 8 (c) reveal that the twist angle is a maximum near the bottom surface at the edge of the electrodes, while it is at a maximum around the mid-cell gap at the centre of the electrodes. The twist angle increases but the tilt angle remains almost the same on increasing the voltage, see figures 8 (b) and 8 (d). This suggests that the transmittance is determined mainly by the twist angle α.

Figure 9 shows the distribution of the LC director for two different voltages, 4.5 and 5.5 V, and a cell gap of 5.6 μm with −LC. As is clearly seen in figures 9 (a) and 9 (c), the twist angle of the LCs increases significantly at 4.5 and 5.5 V compared with those of the cell with $d=3$ μm, while the tilt angle is barely reduced. This indicates that the twist deformation is much easier for the cell with a large cell gap than for one with a low cell gap, and that the degree of upward tilt of the LC is little effected by the cell gap. Consequently, the cell with the lower cell gap requires a higher driving voltage to deform the LC to approximately the same degree compared with the cell with a higher cell gap.

Figure 10 shows the distribution of the LC director at two different voltages, 4.0 and 5.5 V, and a cell gap of 3 μm with the +LC. Considering the twist angles in figures 10 (a) and 10 (c), the maximum twist angle is about the same as that seen for the −LC at the edge of the electrode for the same cell gap, however it is much lower, ranging between 20° and 30° at the centre of the electrode compared with the values of between 40° and

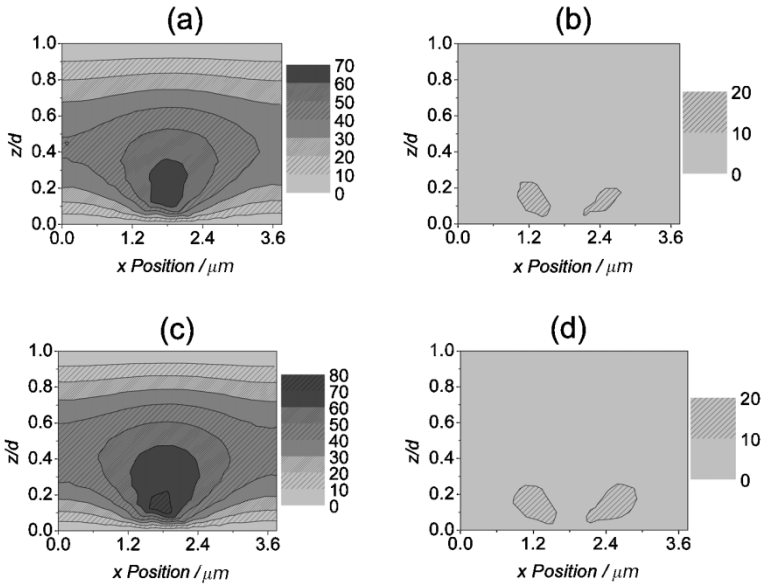

Figure 8. Director profile of the −LC inside the cell along the *y*-axis with a cell gap of 3 μm: twist angle at (*a*) 4.5 V and (*c*) 5.5 V, and tilt angle at (*b*) 4.5 V and (*d*) 5.5 V.

50° for the cell with the −LC, implying lower transmittance for the cell with +LC than that with −LC. Furthermore, the region with a twist angle between 20° and 30° is reduced when the voltage is increased to 5.5 V at the centre of the electrode, which is different behaviour from that seen for the −LC. This results from the increase in the tilt angle with the increasing voltage between the edge and centre of the electrodes, as shown in figures 10 (*b*) and 10 (*d*), thereby effecting less twist force on the LCs at the centre of the electrode. Increasing the tilt angle means that the effective cell retardation value drops, resulting in low transmittance, notwithstanding an increase of the twist angle between the edge and the centre of the electrodes. Consequently, the transmittance at 4.0 V is higher than that at 5.5 V due to the high twist and low tilt angles at 4 V, i.e. the V_{op} is close to 4.0 V.

Next, an investigation of what happens when the cell

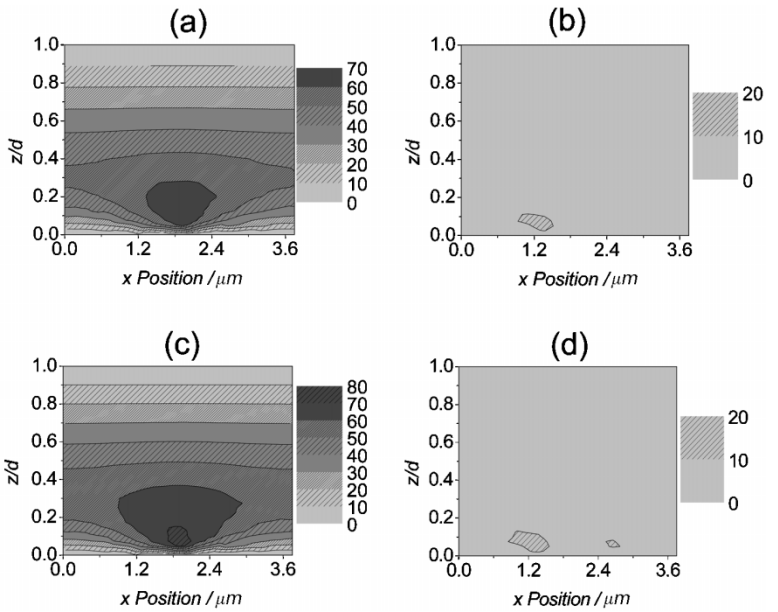

Figure 9. Director profile of the −LC inside the cell along the *y*-axis for a cell gap of 5.6 μm: twist angle at (*a*) 4.5 V and (*c*) 5.5 V, and tilt angle at (*b*) 4.5 V and (*d*) 5.5 V.

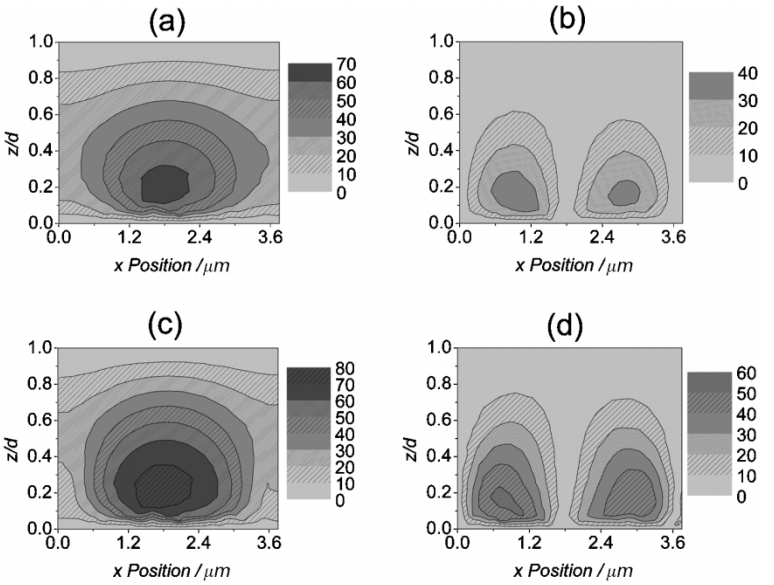

Figure 10. Director profile of the +LC inside cell along *y*-axis for a cell gap of 3 μm: twist angle at (*a*) 4.0 V and (*c*) 5.5 V, and tilt angle at (*b*) 4.0 V and (*d*) 5.5 V.

gap is increased to 4.6 μm was performed. As shown in figure 11, the twist angle increased with increasing voltage in most regions except for a slightly reduced region at the centre of the electrode and the region with a tilt angle between 10° and 20° which remained below $z/d=0.5$ at 5.5 V. This indicates that the transmittance increases slightly when the voltage increases from 4.0 to 5.5 V, implying that the V_{op} is over 4.0 V.

From the analysis of the transmittance distribution and the LC director profile inside the cell, we can understand that in the FFS mode the cell gap-dependent *V–T* characteristics are dependent on the dielectric anisotropy. This is due to the use of a fringe electric field that has both horizontal and vertical components, unlike the IPS mode which uses only a horizontal field. In the IPS mode, the cell gap-dependent *V–T* characteristics are the same for both types of LC since the device is driven by only

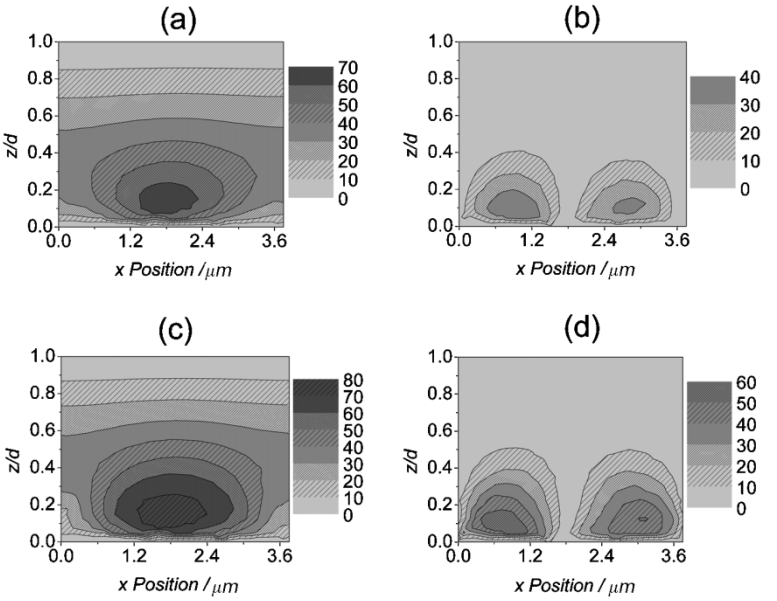

Figure 11. Director profile of the +LC inside the cell along *y*-axis for a cell gap of 4.6 μm: twist angle at (*a*) 4.0 V and (*c*) 5.5 V, and tilt angle at (*b*) 4.0 V and (*d*) 5.5 V.

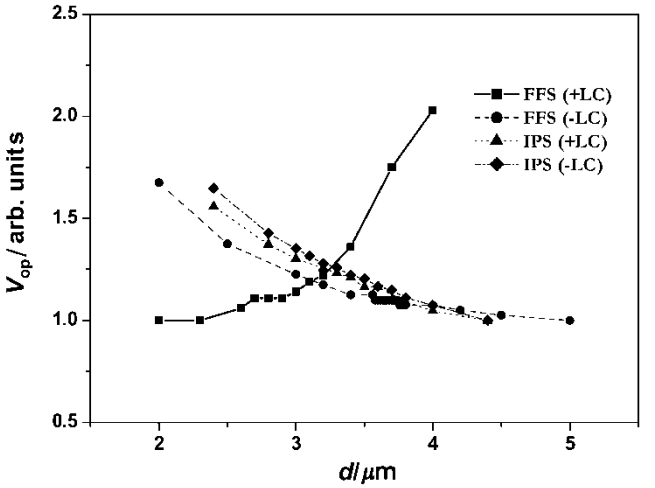

Figure 12. Cell gap-dependent operating voltage in the IPS and the FFS mode depending on dielectric anisotropy of the LC.

the in-plane field. Figure 12 summarizes these characteristics. The FFS mode with −LC, and the IPS mode with +LC and −LC, reveal similar relationships between d and V_{op}, however the FFS mode with +LC shows an inverse relationship.

4. Summary

In summary, we have studied the voltage-dependent transmission characteristics of the FFS mode as a function of the cell gap through simulation and experiment. The results show that in the FFS mode the operating voltage increases with decreasing cell gap for the −LC, whereas it decreases with decreasing cell gap for the +LC. The dependency of the voltage-dependent transmission on dielectric anisotropy of the LC is due to the use of a fringe electric field that deforms the LC in different ways depending on the type of LC. This result is very important in designing an FFS-LCD with a fast response time, high brightness and low power consumption.

This work was in part performed by the Advanced Backbone IT development project supported by the Ministry of Information & Communication in the Republic of Korea.

References

[1] Soref, R. A., 1974, *J. appl. Phys.*, **45,** 5466.
[2] Kiefer, R., Weber, B., Windscheid, F., and Baur, G., 1992, in Proceedings of the 12th International Display Research Conference, Hiroshima, Japan, p. 547.
[3] Oh-e, M., Ohta, M., Aratani, S., and Kondo, K., 1995, in Proceedings of the 15th International Display Research Conference, Hamamatsu, Japan, p. 577.
[4] Mishima, Y., Nakayama, T., Suzuki, N., Ohta, M., Endoh, S., Iwakabe, Y., and Kagawa, H., 2000, *SID Dig.*, 260.
[5] Hong, S. H., Kim, H. Y., Lee, M. H., and Lee, S. H., 2002, *Liq. Cryst.*, **29,** 315.
[6] Lee, S. H., Lee, S. L., and Kim, H. Y., 1998, in Proceedings of the 18th International Display Research Conference, Seoul, Korea, p. 371.
[7] Lee, S. H., Lee, S. L., and Kim, H. Y., 1998, *Appl. Phys. Lett.*, **73,** 2881.
[8] Lee, S. H., Lee, S. L., Kim, H. Y., and Eom, T. Y., 1999, *SID Dig.*, 202.
[9] Lee, S. H., Kim, H. Y., and Lee, S. L., 1999, in Proceeding 6th International Display Workshops, Sendai Japan, p. 191.
[10] Lee, S. H., Lee, S. L., Kim, H. Y., and Eom, T. Y., 1999, *J. Kor. phys. Soc.*, **35,** S1111.
[11] Hong, S. H., Park, I. C., Kim, H. Y., and Lee, S. H., 2000, *Jpn. J. appl. Phys.*, **39,** L527.
[12] Kim, H. Y., Jeon, G. R., Lee, M. H., and Lee, S. H., 2002, *Jpn. J. appl. Phys.*, **41,** 2944.